Simulation Model for the Emulsion Copolymerization of Acrylonitrile and Styrene in Azeotropic Composition

CHEN-CHONG LIN, HWAR-CHING KU, and WEN-YEN CHIU,
Department of Chemical Engineering, National Taiwan University, Taipei, Taiwan, China

Synopsis

A simulation model based on the "unit segment" concept which provides prediction of conversion and molecular weight of product, is proposed for the emulsion polymerization of AN and St in azeotropic composition. Effects of initiator concentration and emulsifier concentration on conversion and molecular weight were studied experimentally and theoretically. It is found that the desorption of AN radicals should be taken into account, and the number of radicals per particle is always less than 0.5. The concentration of polymer particles is proportional to the 0.58 power in respect of the emulsifier concentration and to the 0.35 power in respect of the initiator concentration. The auto-acceleration effect becomes significant when both initial emulsifier concentration and initiator concentration decrease, which influences the average molecular weight of the products. The azeotropic composition of AN–St is 28.5:71.5 by weight for this system at 60°C reaction temperature.

INTRODUCTION

Emulsion polymerization is a heterogeneous reaction where the number of polymer particles generated in the course of the reaction is connected with the progress of polymerization. This kinetic model of the emulsion polymerization has received great attention recently.[1–4] In contrast to emulsion homopolymerization, the kinetics of the emulsion copolymerization have not been studied, primarily because of the complicated mechanism involved in such systems. Nomura[5] proposed a kinetic model of the emulsion copolymerization of styrene (St) and methyl methacrylate (MMA) which could not adequately predict both the conversion and the molecular weight of products. A simulation model for the solution copolymerization of acrylonitrile (AN) and styrene (St) in azeotropic composition based on the "unit segment" concept has been proposed by us in our previous article.[6] The present work proposes a simulation model for the emulsion copolymerization of AN and St in azeotropic composition based on the principle of the generating particles for an emulsion polymerization and "unit segment" concept for a copolymerization. This model predicts adequately the conversion–time data and molecular weight of products for such systems.

KINETIC MODEL OF EMULSION COPOLYMERIZATION

A kinetic model of emulsion copolymerization is summarized by the following mechanisms:

Journal of Applied Polymer Science, Vol. 26, 1327–1342 (1981)
 CCC 0021-8995/81/041327-16$01.60

Initiation:

$$I \xrightarrow{K_{df}} 2I_w^* \quad \text{(decomposition of radicals in water phase)}$$

$$M_p + I_w^* \xrightarrow{K_{e1}} R_1^*$$

$$M_p + M_{aw}^* \xrightarrow{K_{ea}} R_2^* \quad \text{(activation of the polymer particles by entry of radicals from water phase)}$$

$$M_p + M_{bw}^* \xrightarrow{K_{eb}} R_2^*$$

Propagation:

$$X_j^* + M_{ap} \xrightarrow{K_{paa}} X_{j+1}^*$$

$$Y_j^* + M_{ap} \xrightarrow{K_{pba}} X_{j+1}^* \quad \text{(propagation within the polymer particles)}$$

$$X_j^* + M_{bp} \xrightarrow{K_{pab}} Y_{j+1}^*$$

$$Y_j^* + M_{bp} \xrightarrow{K_{pbb}} Y_{j+1}^*$$

Chain transfer:

$$X_j^* + M_{ap} \xrightarrow{K_{faa}} P_j + X_1^*$$

$$Y_j^* + M_{ap} \xrightarrow{K_{fba}} P_j + X_1^* \quad \text{(chain transfer to monomer within the particles)}$$

$$X_j^* + M_{bp} \xrightarrow{K_{fab}} P_j + Y_1^*$$

$$Y_j^* + M_{bp} \xrightarrow{K_{fbb}} P_j + Y_1^*$$

Termination:

$$R_j^* + I_w^* \xrightarrow{K_{e1}} P_j$$

$$R_j^* + M_{aw}^* \xrightarrow{K_{ea}} P_{j+1} \quad \text{(instantaneous termination by radicals from water phase)}$$

$$R_j^* + M_{bw}^* \xrightarrow{K_{eb}} P_{j+1}$$

Desorption:

$$X_1^* \xrightarrow{K_{Dam}} M_{aw}^* \quad \text{(desorption of radicals out of the polymer particles)}$$

$$Y_1^* \xrightarrow{K_{Dbm}} M_{bw}^*$$

where $M_p = M_{ap} + M_{bp}$ and $R_j^* = X_j^* + Y_j^*$.

The symbols used are defined in the Nomenclature. On the basis of the foregoing set of reactions, a mass balance of initiator, monomer, and polymer radical can be obtained. The basic hypotheses made on the derivation of the mass balance equation for an emulsion copolymerization are that (1) initiation, propagation, and termination all take place in the polymer particles; (2) diffusion

processes of free radicals of initiator and monomer are not the controlling steps of the reaction; (3) a polymer particle contains not more than one polymerizing radical; (4) instantaneous termination takes place when the second radical enters the particle which contains a radical; (5) only monomer radicals can escape and enter the particles; and (6) reaction in the water phase is considered negligible.

In considering the desorption process, we assume for a first approximation that

$$K_{Dam}[X_1^*] \simeq K_{Da}X_T \qquad \text{and} \qquad K_{Dbm}[Y_1^*] \simeq K_{Db}Y_T \tag{1}$$

where $X_T = \Sigma_{j=1}^{\infty}[X_j^*]$, $Y_T = \Sigma_{j=1}^{\infty}[Y_j^*]$, and K_{Da} is a new rate constant as defined in eq. (1). Under steady-state conditions, the following equation will be valid:

$$(K_{pba} + K_{fba})[M_{ap}]Y_T = (K_{pab} + K_{fab})[M_{bp}]X_T \tag{2}$$

In general, $K_p \gg K_f$, and eq. (2) becomes

$$K_{pba}[M_{ap}]Y_T = K_{pab}[M_{bp}]X_T \tag{3}$$

From the mass balance equations, the following relation will be obtained:

$$\left(\frac{r_i}{N} + K_{Da}\bar{n}_a + K_{Db}\bar{n}_b - \frac{1}{N}\frac{dN}{dt}\right)(1 - 2\bar{n}_t) = k_{Da}\bar{n}_a + K_{Db}\bar{n}_b - \frac{1}{N}\frac{dN}{dt} \tag{4}$$

where $\bar{n}_t = R_T/N$, $\bar{n}_a = X_T/N$, and $\bar{n}_b = Y_T/N$. Solution of eq. (4) for $\bar{n}_t$ gives

$$\bar{n}_t = \tfrac{1}{2}[-(CD - ED) + \{(CD - ED)^2 + 2CD\}^{1/2}] \tag{5}$$

where $A = \bar{n}_b/\bar{n}_a$, $C = r_i/K_{Da}N$, $E = (dN/dt)/K_{Da}N$, $D = (1 + A)/(1 + AB)$, $B = K_{Db}/K_{Da}$, $\bar{n}_a = 1/(1 + A)\bar{n}_t$, $\bar{n}_b = A/(1 + A)\bar{n}_t$, and

$$A = \frac{\bar{n}_b}{\bar{n}_a} = \frac{K_{paa}}{K_{pbb}}\frac{\gamma_b}{\gamma_a}\frac{[M_{bp}]}{[M_{ap}]} \tag{6}$$

Beyond the induction period where dN/dt becomes zero, eq. (5) reduces to

$$\bar{n}_t = \tfrac{1}{2}(-CD + [(CD)^2 + 2CD]^{1/2}] \tag{7}$$

According to our concept of "unit segment," [6] the process of an azeotropic copolymerization can now be simplified to the following homopolymerization scheme, which is mathematically more manageable:

Initiation:

$$I \xrightarrow{K_{df}} 2I_w^*$$

$$M_p + I_w^* \xrightarrow{K_{el}} R_1^*$$

$$M_p + M_w^* \xrightarrow{K_t} R_2^*$$

Propagation:

$$R_j^* + M_p \xrightarrow{K_p} R_{j+1}^*$$

Chain transfer:

$$R_j^* + M_p \xrightarrow{K_{fm}} P_j + R_1^*$$

Termination:

$$R_j^* + I_w^* \xrightarrow{K_{eI}} P_j$$

$$R_j^* + M_w^* \xrightarrow{K_t} P_{j+1}$$

Desorption:

$$R_1^* \xrightarrow{K_{Dm}} M_w^*$$

where $M_w^* = M_{aw}^* + M_{bw}^*$.

In the above desorption process, the following assumption is also valid:

$$K_{Dm}[R_1^*] \simeq K_D R_T \tag{8}$$

where K_D is a new rate constant as defined in eq. (8). On the basis of the foregoing set of reactions, the simplified mass balance equations of initiator, monomer, and polymer radicals are obtained, and the following relation can be easily derived for the copolymer composition equation of this system:

$$\frac{d[M_a]}{d[M_b]} = \frac{K_{paa}[M_{ap}]X_T + K_{pba}[M_{ap}]Y_T}{K_{pbb}[M_{bp}]Y_T + K_{pab}[M_{bp}]X_T} = \frac{[M_{ap}]}{[M_{bp}]} \frac{\gamma_a[M_{ap}] + [M_{bp}]}{\gamma_b[M_{bp}] + [M_{ap}]} \tag{9}$$

At azeotropic composition, eq. (9) reduces to

$$\frac{\gamma_a[M_{ap}] + [M_{bp}]}{\gamma_b[M_{bp}] + [M_{ap}]} = 1 \tag{10}$$

For the rate of copolymerization, eq. (9) gives

$$K_p = \frac{K_{paa}\left(C_a + \frac{C_b}{\gamma_a}\right)\bar{n}_a + K_{pbb}\left(C_b + \frac{C_a}{\gamma_b}\right)\bar{n}_b}{\bar{n}_t} \tag{11}$$

$$K_t = \frac{K_{ea}[M_{aw}^*] + K_{eb}[M_{bw}^*]}{[M_{aw}^*] + [M_{bw}^*]} \tag{12}$$

$$K_D = K_{Da}\bar{n}_a + K_{Db}\bar{n}_b \tag{13}$$

$$K_{fm} = \frac{K_{faa}C_a\bar{n}_a + K_{fab}C_b\bar{n}_a + K_{fba}C_a\bar{n}_b + K_{fbb}C_b\bar{n}_b}{\bar{n}_t} \tag{14}$$

where C_a and C_b are the mole fractions of AN and St in the oil phase, respectively. The values of K_p, K_t, K_D, and K_{fm} in the above equations are all constants; they do not change with reaction time and are obtainable experimentally.

It is well known that the path of an emulsion polymerization can be divided into three reaction periods: induction, zero-order reaction, and first-order reaction. The kinetic analysis of this system is accomplished for each reaction stage as follows:

Induction Period ($0 \leq t < t_{in}$, or $0 \leq x < x_{in}$)

In this period, $[M_p] = [\hat{M}_p]$:

$$R_{pi} = \frac{-d[M]}{dt} = K_p[\hat{M}_p]\bar{n}_t N + K_{fm}[\hat{M}_p]\bar{n}_t N \tag{15}$$

Since $K_{fm}/K_p = 10^{-5} \sim 10^{-6}$ and the second term on the right side of eq. (15) is negligible, the equation reduces to

$$R_{pi} = K_p[\overline{M}_p]\bar{n}_t N \tag{16}$$

where the value of $\bar{n}_t$ is obtainable from eq. (5). The conversion is defined as

$$x = \frac{53([M_{ao}] - [M_a]) + 104([M_{bo}] - M_b])}{53([M_{ao}] - [M_{aw}]) + 104([M_{bo}] - [M_{bw}])} \tag{17}$$

where $[M_{bo}]$ and $[M_{ao}]$ indicate the initial concentrations of St and AN, respectively, and $[M_{bw}]$ and $[M_{aw}]$ indicate the concentrations of St and AN dissolved in the water phase, respectively. The conversion is now simulated by the following equation:

$$x = \frac{[M_{ao}] - [M_a]}{[M_{ao}] - [M_{aw}]} = \frac{[M_{bo}] - [M_b]}{[M_{bo}] - [M_{bw}]} = \frac{[M_o] - [M]}{[M_o] - [M_{aw}] - [M_{bw}]} = \frac{1}{[M_o] - [M_{aw}] - [M_{bw}]} \int_0^t R_{pi}\, dt$$

Zero-Order Period ($t_{in} \leq t < t_{en}$ or $x_{in} \leq x < x_{en}$)

In this period, $dN/dt = 0$, $N = \hat{N}$, and $[M_p] = [\hat{M}_p]$, a constant value. Namely,

$$R_{pz} = K_p\bar{n}_t[\hat{M}_p]\hat{N} \tag{19}$$

where the value of $\bar{n}_t$ is obtainable from eq. (7). The conversion is written as

$$x = x_{in} + \frac{R_{pz}}{[M_o] - [M_{aw}] - [M_{bw}]}(t - t_{in}) \tag{20}$$

First-Order Period ($t \geq t_{en}$ or $x \geq x_{en}$)

This period is characterized by the two facts: (1) $N = \hat{N}$ and (2) the monomer droplets all disappear and the monomer concentration in the polymer particles decreases gradually as it consumes them.
Thus,

$$R_{pf} = K_p\bar{n}_t[M_p]\hat{N} = K_p\phi([M] - [M_{aw}] - [M_{bw}])\bar{n}_t\hat{N} \tag{21}$$

where

$$\phi = \frac{[M_p]}{[M] - [M_{aw}] - [M_{bw}]} = \frac{[\hat{M}_p]}{([M_o] - [M_{aw}] - [M_{bw}])(1 - x_{en})}$$

which means the reciprocal of the volume fraction of polymer particles in reaction mixture.

For the conversion, it gives

$$x = -(1 - x_{en})\exp[-\bar{n}_t \phi K_p \hat{N}(t - t_{en})] + 1 \tag{22}$$

Now for the degree of polymerization, the following equations are developed:

$$\frac{d[\mathrm{P}_j]}{dt} = K_{fm}[\mathrm{R}_j^*][\mathrm{M}_p] + K_{eI}[\mathrm{I}_w^*][\mathrm{R}_j^*] + K_t[R_{j-1}^*][\mathrm{M}_w^*] \tag{23}$$

and

$$\frac{d\hat{\mathrm{P}}}{dt} = K_{fm}[\mathrm{M}_p]R_T + K_{eI}[\mathrm{I}_w^*]R_T + K_t[\mathrm{M}_w^*]R_T \tag{24}$$

Assuming $[R_{j-1}^*] \simeq [R_j^*]$,

$$\frac{d[\mathrm{P}_j]}{dt} \propto [R_j^*] \qquad \text{and} \qquad \frac{d\hat{\mathrm{P}}}{dt} \propto R_T$$

where $\hat{\mathrm{P}} = \Sigma_{j=1}^{\infty}[\mathrm{P}_j]$.

According to the definition, the viscosity-average degree of polymerization of polymer radicals can be expressed as

$$\bar{P}_\mu^*(t) = \left(\frac{\sum_{j=2}^{\infty} j^{1+a}[\mathrm{R}_j^*]}{\sum_{j=2}^{\infty} j[\mathrm{R}_j^*]}\right)^{1/a} = \left(\frac{\sum_{j=2}^{\infty} j^{1+a}\beta^{j-2}[\mathrm{R}_2^*]}{\sum_{j=2}^{\infty} j\beta^{j-2}[\mathrm{R}_2^*]}\right)^{1/a} \tag{25}$$

where

$$\frac{1}{\beta} = 1 + \frac{1}{\nu}$$

and

$$\nu = \frac{K_p[\mathrm{M}_p]R_T}{K_{eI}[\mathrm{I}_w^*] + K_{fm}[\mathrm{M}_p] + K_t[\mathrm{M}_w^*]}$$

according to the ν model[7]; and when ν is very large, $\beta \simeq e^{-1/\nu}$. Equation (25) is now reduced to

$$\bar{P}_\mu^*(t) \simeq \left(\frac{\int_o^{\infty} j^{1+a}e^{-j/\nu}dj}{\int_o^{\infty} j\, e^{-j/\nu}dj}\right)^{1/a} = \nu[\Gamma(a+2)]^{1/a} \tag{26}$$

For the viscosity-average degree of polymerization of dead polymer, we obtain

$$\bar{P}_\mu(t) = \left(\frac{\int_o^t \bar{P}_\mu^*(t)^a R_p\, dt}{\int_o^t R_p\, dt}\right)^{1/a} = (\Gamma(a+2))^{1/a}\left(\frac{\int_o^t \nu^a R_p\, dt}{\int_o^t R_p\, dt}\right)^{1/a} \tag{27}$$

which should be divided into three reaction periods as follows:

Induction period:

$$\nu_i = \frac{R_{pi}}{K_d f[\mathrm{I}] + K_{fm}[\hat{\mathrm{M}}_p]\bar{n}_t N} \tag{28}$$

$$\overline{P}_{\mu_i}(t) = [\Gamma(a+2)]^{1/a} \left(\frac{\int_o^t \nu_i^a R_{pi}\, dt}{\int_o^t R_{pi}\, dt} \right)^{1/a}$$

$$= [\Gamma(a+2)]^{1/a} \left(\frac{\int_o^t \nu_i^a R_{pi} dt}{[\mathrm{M}_o] - [\mathrm{M}]} \right)^{1/a} \quad (29)$$

Zero-order period:

$$\nu_z = \frac{R_{pz}}{K_d f[\mathrm{I}] + K_{fm}[\hat{\mathrm{M}}_p]\overline{n}_t \hat{N}} \quad (30)$$

$$\overline{P}_{\mu_z}(t) = \left(\frac{\int_o^{t_{in}} \nu_i^a R_{pi} dt + \int_{t_{in}}^t \nu_z^a R_{pz}\, dt}{[\mathrm{M}_o] - [\mathrm{M}]} \right)^{1/a} [\Gamma(a+2)]^{1/a} \quad (31)$$

First-order period:

$$\nu_f = \frac{R_{pf}}{K_d f[\mathrm{I}] + K_{fm}\phi([\mathrm{M}] - [\mathrm{M}_{aw}] - [\mathrm{M}_{bw}])\overline{n}_t \hat{N}} \quad (32)$$

$$\overline{P}_{\mu_f}(t) = \left(\frac{\int_o^{t_{in}} \nu_i^a R_{pi}\, dt + \int_{t_{in}}^{t_{en}} \nu_z^a R_{pz}\, dt + \int_{t_{en}}^t \nu_f^a R_{pf}\, dt}{[\mathrm{M}_o] - [\mathrm{M}]} \right)^{1/a}$$

$$\times [\Gamma(a+2)]^{1/a} \quad (33)$$

If the numerical values in the above equations are available, the emulsion copolymerization can now be simulated by a computer. Table I lists the experimental conditions and numerical values used for calculation of this simulation model.

EXPERIMENTAL

Materials. Styrene and acrylonitrile were purified by distillation from industrial-grade monomers. The emulsifier used was sodium lauryl sulfate of extra pure grade. Reagent-grade potassium persulfate was used as the initiator.

Emulsion Copolymerization. Emulsion copolymerization was carried out in a four-neck flask equipped with a two-blade paddle-type impeller, four baffle plates, a thermometer, nitrogen inlet, feed inlet, and condenser. The copolymerization was performed under batchwise operation. The experimental conditions are listed in Table I. Conversion was determined by the gravimetric method of solid product precipitated and dried from the reaction mixture.

TABLE I
Polymerization Conditions and Numerical Values in Simulation Model

Condition
[AN] = 0.1425 g/cc H_2O
[St] = 0.3575 g/cc H_2O
Temp. = 60 ± 1°C
Stirring: 400 ~ 450 rpm

Numerical values			Reference
K_{df}	4.8×10^{-6}	sec^{-1}	11
K_{paa}	30,000	l./mole sec	10
K_{pbb}	376	l./mole sec	10
γ_a	0.04	—	a
γ_b	0.44	—	a
ρ_p	1.1078	g/cm^3	10
ρ_m	0.872	g/cm^3	10
C_a	0.368	—	a
C_b	0.632	—	a
K_{fm}/K_p	3.6×10^{-5}	—	b
K_p	873.5	l./mole sec	b
K_{Da}	8	sec^{-1}	b
S_{CMC}	0.42	g/l. H_2O	b

[a] Evaluated from CHN analysis in this work.
[b] Determined experimentally in this work.

Nitrogen content of the polymer products was determined by a CHN Corder (Yanaco MT-2). The average degree of polymerization ($\bar{P}_\mu$) was determined by employing Shimura's equation[8]

$$[\eta] = 3.6 \times 10^{-4}\bar{M}^{0.62} \tag{34}$$

The concentration of polymer particles was determined from the monomer conversion and the diameter of polymer particles measured by a transmission electron microscope (Hitachi HU 12):

$$N = \frac{6\nu_p([M_o] - [M_{aw}] - [M_{bw}])x}{t\bar{d}^3} \tag{35}$$

After separating the remaining monomer droplets in the sample with a centrifuge, the monomer concentration in the polymer particles was measured by weighing the polymer before and after polymerizing the residual monomer in the polymer particles. To follow the progress of polymerization, the surface tension of the aqueous phase free of monomer droplets was also measured by a du Noüy tensiometer.

RESULTS AND DISCUSSION

To clarify the mechanism of the emulsion copolymerization, it is necessary to know in detail the characteristic features of the reaction. For this reason, the monomer conversion (x), the average degree of polymerization ($\bar{P}_\mu$), the surface tension of the aqueous phase (σ), the number of polymer particles (N), and the weight fraction of monomer in the polymer particles (r) were all measured during the polymerization. The number of polymer particles produced is obtainable by electromicroscopic observation.

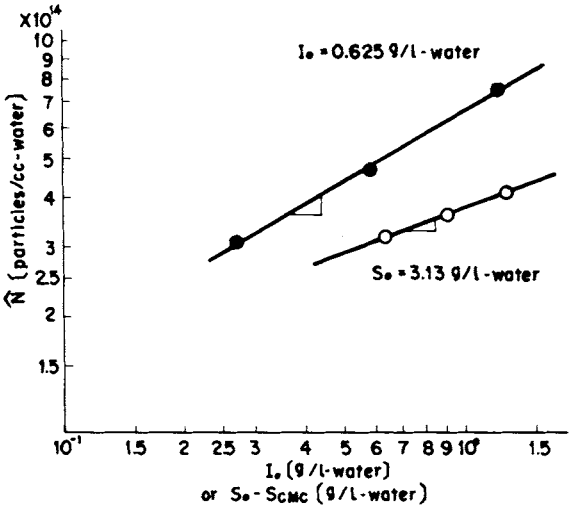

Fig. 1. Relationship between number of particles and emulsifier or initiator concentration.

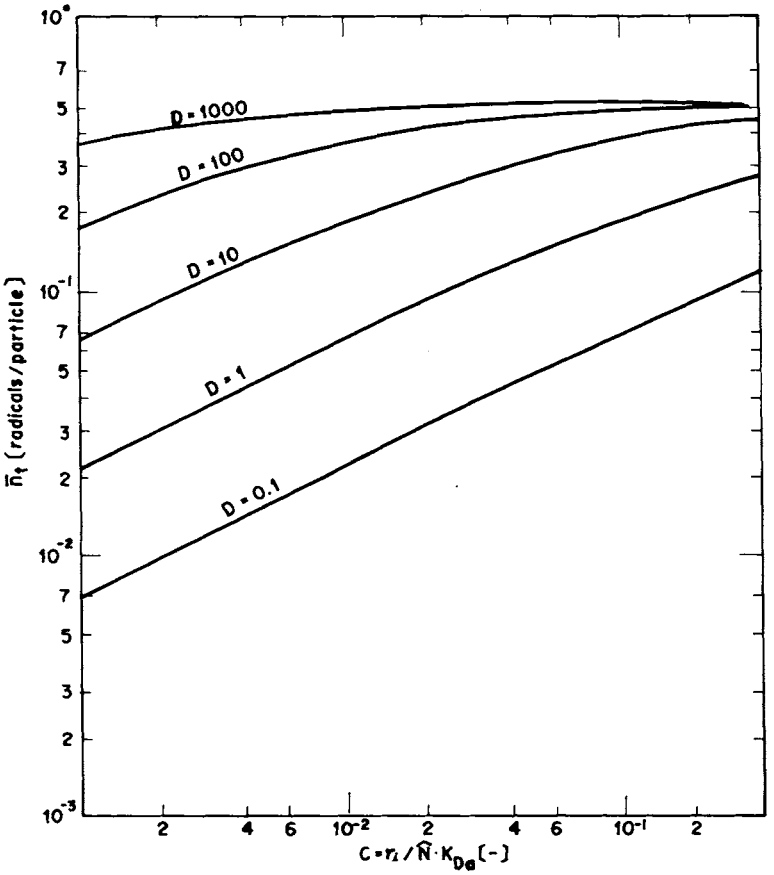

Fig. 2. Plot of average number of radicals per particle vs. $C = r_i/K_{Da}\hat{N}$ of eq. (7).

Figure 1 shows the experimental result of the effects of both emulsifier and initiator concentration on the number of polymer particles. The concentration of the polymer particles is approximately proportional to the 0.58 power in respect of the emulsifier concentration and the 0.35 power in respect of the initiator concentration. Assuming that the rate of particle formation remains constant in the induction period, $N = yt$. The value of the proportionality constant (y) is obtainable by plotting $\hat{N}$ against t_{in}. The plot of the average number of radicals per particle in the zero-order period against parameter $C = r_i(K_{Da}\hat{N})$ in various values of D is shown in Figure 2. It is seen that the value of $\bar{n}_t$ will approach 0.5 when $D \to \infty$ or $C \to \infty$ according to eq. (7). In fact, the value of $A = \bar{n}_b/\bar{n}_a$ of eq. (6) is very large, and, in turn, the polymer radical having the styrene as terminal is predominant. As a result, the desorption process of St monomer radical is negligible (i.e., $K_{Db} \simeq 0$). Therefore, $\bar{n}_t$ will be close to 0.5 in spite of the desorption process of AN monomer radical. This fact is also confirmed experimentally in Figure 3.

Figure 4 shows the theoretical conversion–time curve calculated from eqs. (18),

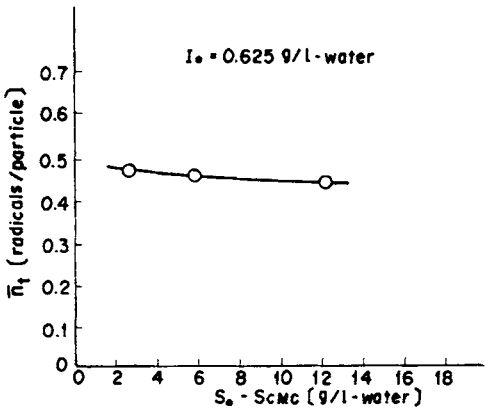

Fig. 3. Effect of emulsifier concentration on number of radicals per particle.

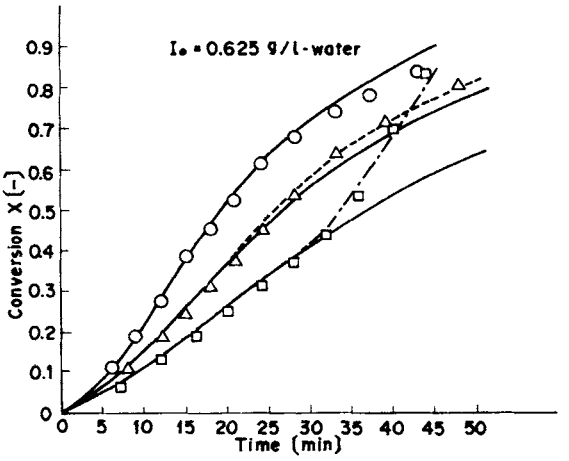

Fig. 4. Theoretical and experimental conversion–time curves with various emulsifier concentrations. Dotted curves indicate the calculated results with autoacceleration by eq. (36) at a constant I_0 = 0.625 (g/l. water). Experimental data: S_0 = 3.13 (□), 6.25 (△), 12.5 (○) (g/l. water)

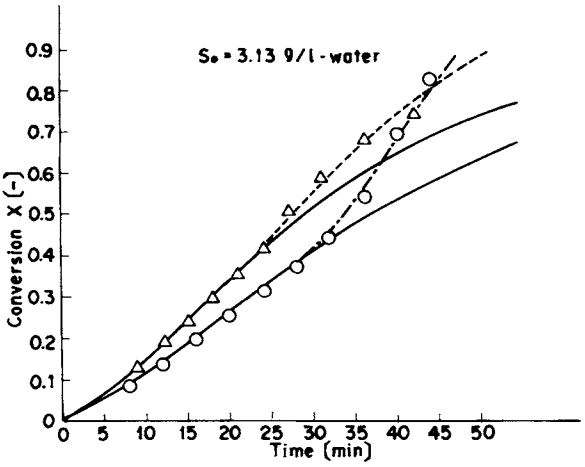

Fig. 5. Theoretical and experimental conversion–time curves with two different initiator concentrations. Dotted curves indicate the calculated results with autoacceleration by eq. (36) at a constant S_o = 3.13 (g/l. water). Experimental data: I_o = 1.25 (△) and 0.625 (○) (g/l. water).

(20), and (22). Autoacceleration effects are evident in the case of low emulsifier concentration. Therefore, the simulation model is modified by the following equation:

$$R_{pa} = R_{pf}[1 + \alpha(x - x_a)] \tag{36}$$

where R_{pa} is the rate of polymerization with the autoacceleration; R_{pf}, the rate of polymerization without the autoacceleration; according to eq. (21), α, the correction factor; and x_a, the conversion at the point of occurrence of the autoacceleration.

Figure 5 shows the conversion–time curve in two different initiator concentrations. The correction factor (α) can be obtained experimentally as shown in Figure 6. The theoretical curves agree well with the experimental data in both cases. An example of the relationships among the surface tension, conversion,

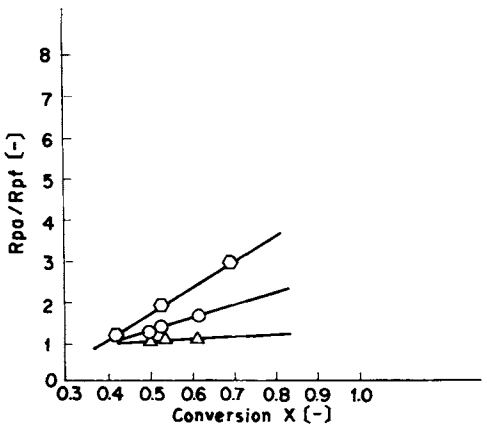

Fig. 6. Experimental determination of correction factors for autoacceleration: (○) I_o = 0.625 (g/l. water), S_o = 3.13 (g/l. water); (○); I_o = 1.25 (g/l. water), S_o = 3.13 (g/l. water); (△) I_o = 0.625 (g/l. water), S_o = 6.25 (g/l. water).

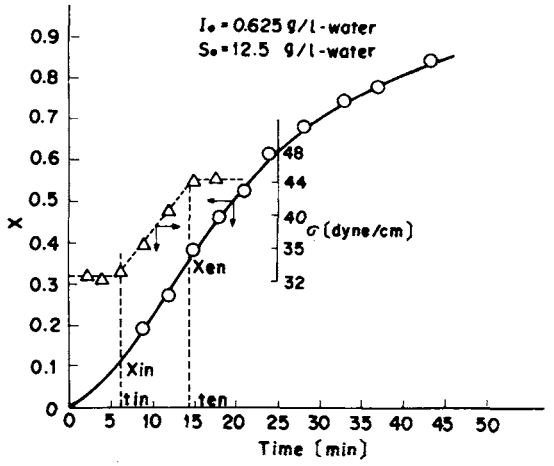

Fig. 7. Relationship among surface tension, conversion, and reaction time. Figure describes the points of x_{in} and x_{en}.

and time is shown in Figure 7. In the polymerization course, the surface tension (σ) remains constant in the induction period, but when the conversion reaches $x = x_{in}$, the surface tension begins to increase sharply up to $x = x_{en}$; thereafter the surface tension keeps constant again. Figure 8 shows the weight fraction of monomer in the polymer particles (r). The value of r is nearly constant in the range $x < 0.39$, and the variation of r with conversion x can be expressed by the equation $r = 1 - x$ in the range $x > 0.39$. These experimental results indicate that monomer droplets exist in the range $x < 0.39$, while in the range $x > 0.39$ the number of polymer particles and the total volume of polymer particles remain almost constant. Hence, the surface tension remains unaltered.

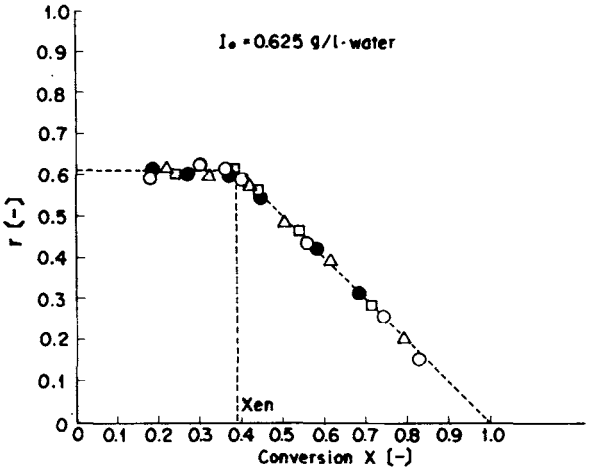

Fig. 8. Relationship between monomer weight fraction in monomer-swollen polymer particles and conversion at constant I_o = 0.625 (g/l. water). Experimental data: S_o = 25 (△), 12.5 (●), 6.25 (□), 3.13 (○) (g/l. water). Figure describes the point of x_{en}.

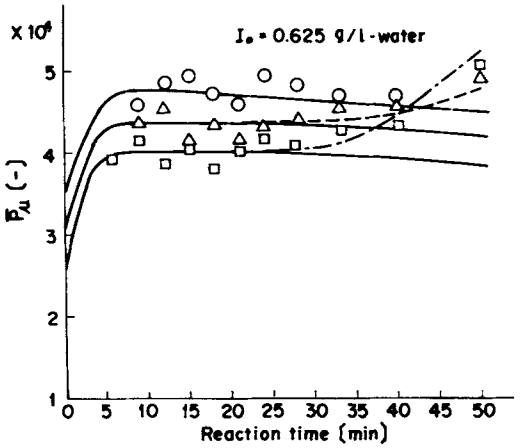

Fig. 9. Comparison of calculated $\bar{P}_\mu$ with experimental $\bar{P}_\mu$ vs. reaction times at constant $I_0 = 0.625$ (g/l. water). Experimental data: $S_0 = 12.5$ (○), 6.25 (△), 3.13 (□) (g/l. water).

The variation of the viscosity-average degree of polymerization ($\bar{P}_\mu$) as a function of time can be evaluated theoretically from eqs. (29), (31), and (33). Figure 9 and 10 show both theoretical and experimental results of the viscosity-average degree of polymerization. The dotted lines indicate the theoretical calculations based on the autoacceleration effects. It is evident that the polymer molecular size is affected by the autoacceleration effects because of the increase in the rate of reaction as indicated in eq. (36). The emulsion polymerization of a partially water-soluble monomer such as acrylonitrile or vinyl acetate may be characterized by the desorption process. It is also observed that the rate of copolymerization of this system is not exactly proportional to the number of polymer particles, indicating the occurrence of this desorption process. A value of $K_{Da} = 8[\text{sec}^{-1}]$ for the desorption rate constant of AN in the theoretical calculation fits well with the experimental results (Fig. 11). If we consider the

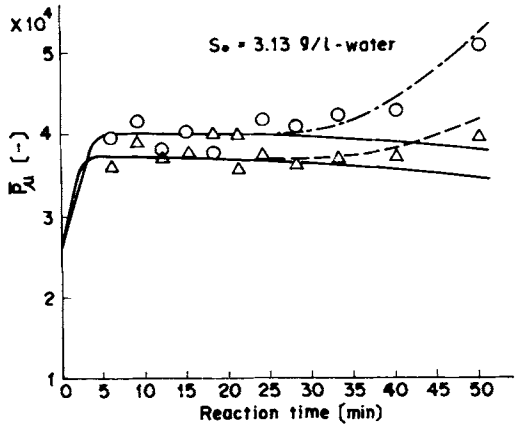

Fig. 10. Comparison of calculated $\bar{P}_\mu$ with experimental $\bar{P}_\mu$ vs. reaction time at constant $S_0 = 3.13$ (g/l. water). Experimental data: $I_0 = 1.25$ (○), 0.625 (△) (g/l. water).

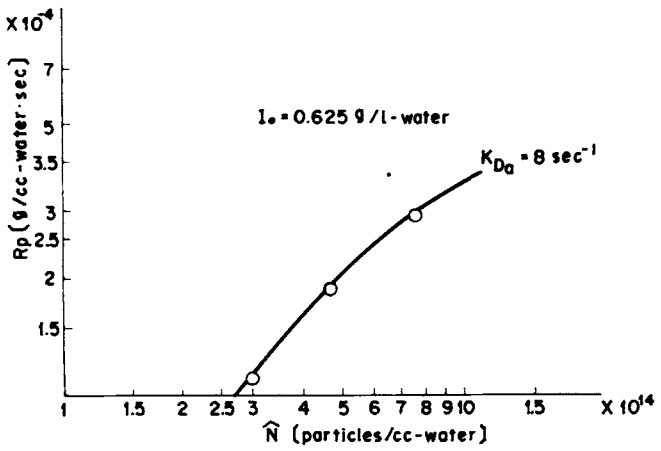

Fig. 11. Effect of number of polymer particle on reaction rate. A value of K_{Da} = 8 (sec^{-1}) fits well with experimental curve.

degree of polymerization of products at the zero-order period, eq. (31) reduces approximately to eq. (37):

$$\bar{P}_{\mu_z}(t) = [\Gamma(a+2)]^{1/a}\nu \tag{37}$$

Rearrangement of eq. (37) leads to eq. (38):

$$\frac{[\Gamma(a+2)]^{1/a}}{\bar{P}_{\mu_z}(t)} = \frac{K_{fm}}{K_p} + \frac{K_d f}{K_p[\hat{M}_p]\bar{n}_t}\frac{[I]}{\hat{N}} \tag{38}$$

A graph of $\{[\Gamma(a+2)]^{1/a}\}/\bar{P}_{\mu_z}(t)$ $[I]/\hat{N}$ should give a straight line with an intercept of K_{fm}/K_p. Because [I] remains approximately constant during the polymerization, we plot $[I_o]$ instead of [I] in Figure 12. A value of $K_{fm}/K_p = 3.6 \times 10^{-5}$ was obtained from the plot of Figure 12.

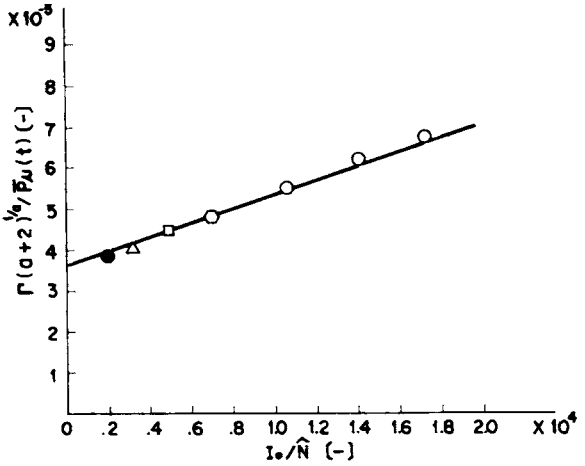

Fig. 12. Plot of $\Gamma(a+2)^{1/a}/\bar{P}_{\mu_z}(t)$ vs. $I_o/\hat{N}$. I_o = 0.625 (g/l. water): S_o = 12.5 (g/l. water) (●), 6.25 (△), 3.13 (□). I_o = 1.25 (g/l. water): S_o = 3.13 (g/l. water) (○), 3.13 (seeded) (○). A value of $K_{fm}/K_p = 3.6 \times 10^{-5}$ was obtained as an intercept.

TABLE II
CHN Analysis of Copolymer Samples[a]

Monomer AN:St, wt %	Time, min	C %	H %	N %	Copolymer AN:St, mole %
25:75	10	86.79	7.79	5.42	33.6:66.4
	20	86.57	7.83	5.60	34.5:65.5
	30	86.48	7.72	5.80	35.6:64.4
27.7:72.3	10	86.79	7.59	5.62	34.2:65.8
	20	86.61	7.65	5.74	35.3:64.7
	30	86.57	7.57	5.86	35.9:64.1
28.5:71.5	10	86.33	7.64	6.03	36.7:63.3
	20	86.29	7.65	6.06	36.9:63.1
	30	86.34	7.62	6.04	36.8:63.2

[a] Temperature 60°C, $[I_o]$ = 0.625 g/l. water, $[S_o]$ = 12.5 g/l. water.

Table II shows a typical example of the CHN analysis of products in various monomer feed compositions. For AN–St emulsion copolymerization, an azeotropic mixture of AN:St = 28.5:71.5 by weight is found for such polymerization condition. Taking the condition of $[M_o]$ = 500 g/l. H_2O, the calculated acrylonitrile concentration in the water phase from the data of Table II will be 36.4 g/l. H_2O, which agrees well with the value of 35.4 g/l. H_2O given by Smith[9] in the equilibrium volume measurement.

All of the experimental data are in good agreement with the theoretical predictions. This confirms the validity of our mathematical model of emulsion copolymerization given in this work.

NOMENCLATURE

f	efficiency of initiator
I	initiator
K	rate constant
M	monomer
$\bar{n}_t$	number of radicals per polymer particle
N	number of polymer particles (mole/l) or (particles/cm^3 water)
P	dead polymer
$\hat{P}$	total concentration of dead polymer (mole/l.)
$\bar{P}_\mu$	viscosity-average degree of dead polymer
$\bar{P}^*_\mu$	viscosity-average degree of polymer radicals
R_T	total concentration of polymer radicals (mole/l.)
R_P	rate of propagation (mole/l. sec or g/cm^3 water sec)
r	weight fraction of monomer in polymer particles
S	emulsifier
S_{CMC}	critical micelle concentration (g/l. H_2O)
t_{in}	time at $x = x_{in}$ (min)
t_{en}	time at $x = x_{en}$ (min)
x_{in}	conversion at the time when the reaction shifts from the induction period to the zero-order period
x_{en}	conversion at the time when the reaction shifts from the zero-order period to the first-order period
x_a	conversion at the time when autoacceleration occurs
X^*_j	polymer radical having AN terminal
Y^*_j	polymer radical having St terminal

Greek Letters

ρ density (g/cm^3)
γ monomer reactivity ratio
ν_p specific volume of polymer (cm^3/g)

Subscripts

a acrylonitrile
b styrene
d initiator decomposition
D desorption in homo-scheme
eI initiation or termination
f chain transfer or first-order period
fm chain transfer in homo-scheme
i induction period
m monomer
o initial
p of polymer particle or propagation
t termination
w of water phase
z zero-order period

References

1. C. P. Roe, *Ind. Eng. Chem.*, **60,** 20 (1968).
2. J. L. Gardon, *J. Polym. Sci., Part A-1, 6,* 623 (1968).
3. S. Omi, Y. Shiraishi, H. Sato, and H. Kubota, *J. Chem. Eng. Jpn.*, **2,** 64 (1969).
4. M. Harada, M. Nomura, H. Kojima, W. Eguchi, and S. Nagata, *J. Appl. Polym. Sci.*, **16,** 811 (1972).
5. M. Nomura, *Polymer Colloid Group Newsletter*, 1978.
6. C. C. Lin, W. Y. Chiu, and C. T. Wang, *J. Appl. Polym. Sci.*, **23,** 1203 (1979).
7. Y. Iwasa, S. Rhee, and T. Imoto, *Kagaku Kogaku*, **31,** 373 (1967).
8. Y. Shimura, I. Mita, and H. Kamoe, *J. Polym. Sci.*, $\mathbf{B}_2$, 403 (1964).
9. W. V. Smith, *J. Am. Chem. Soc., 71,* 5, 4077 (1949).
10. J. Brandrup and E. H. Immergut, Eds., *Polymer Handbook*, 2nd ed., Wiley, New York, 1975.
11. F. A. Bovey and I. M. Kolthoff, *Emulsion Polymerization*, Interscience, New York, 1955.

Received August 6, 1980
Accepted August 29, 1980